The role of pions as virtual constituents of light bound states

Walter Heupel[*]

Justus-Liebig-Universitaet Giessen
E-mail: walter.heupel@theo.physik.uni-giessen.de

Stanislav Kubrak[†]

Justus-Liebig-Universitaet Giessen
E-mail: stanislav.kubrak@physik.uni-giessen.de.

Gernot Eichmann

Karl-Franzens-Universitaet Graz
E-mail: gernot.eichmann@theo.physik.uni-giessen.de

Christian Fischer[‡]

Justus-Liebig-Universitaet Giessen
E-mail: christian.fischer@theo.physik.uni-giessen.de

We summarize recent results for the spectrum and properties of light pseudoscalar and scalar hadrons in a functional approach to QCD using Dyson-Schwinger and Bethe-Salpeter equations. We focus in particular on the role of pions as virtual constituents in light mesons ('pion cloud effects') as well as their role as constituents of tetraquark bound states. An extension of our framework into the charm quark sector reveals an all-charm tetraquark in the mass region around 5.5 GeV.

---

[*]Poster Presentation

[†]Poster Presentation

[‡]Speaker.

1. Introduction

Pions are the lightest hadrons in nature. Their special status as the lightest members of an octet of pseudoscalar (pseudo-)Goldstone bosons associated with the breaking of the $SU(3)_A$ part of chiral symmetry makes them fascinating objects to study. In effective theories, pions appear as elementary degrees of freedom. Naturally, these theories have nothing to say about the internal structure of the pion. Within QCD, however, pions are formed as bound states of a quark and an anti-quark interacting strongly with each other. Powerful constraints such as the axial Ward-Takahashi identity guarantee the massless Goldstone boson nature of the pions in the chiral limit, although the constituents remain massive. This fascinating interplay between dynamical mass generation on the quark level and the formation of massless bound states is particularly transparent in functional approaches to QCD using Dyson-Schwinger, Bethe-Salpeter and Faddeev equations, see e.g. [1 − 4] for reviews.

An important probe for the internal structure of hadrons is their response to electromagnetic fields. Real and virtual photons serve to extract quantities such as form factors, polarizabilities and distribution functions which in turn offer interesting insights into global as well as spatially resolved electromagnetic properties of these hadrons. Virtual pions (the 'pion cloud' [5]) play an important role in this respect. At small momentum transfer, the incoming photons couple dominantly to the virtual pion cloud of the bound state instead of the quark and antiquark constituents. An impressive demonstration of this effect has been given in [6], where the electromagnetic form factors of the nucleon have been determined in a three-body Faddeev approach. A similar picture has been found for the axial and pseudoscalar form factors [7]. The inclusion of pion cloud effects into form factor calculations within the functional approach is challenging, both conceptually and numerically. First steps in this direction have been made in [8, 9], where pion cloud effects in the masses of light mesons have been studied. In this proceedings contribution we report on our efforts to determine meson form factors in this approach.

Another interesting place where virtual pions may play a role are tetraquark bound states. The story of the tetraquark is tightly connected to the issue of the light scalars and especially to the case of the σ meson. Back in the 70ies, Jaffe introduced a simple quark-bag model to describe these states [10]. He showed that tetraquarks allow for a natural explanation for the inverted mass spectra and the huge width found in the lightest 0^+ meson nonet. Unfortunately this huge width and the multitude of other particles with 0^+ quantum numbers in the low mass region made a clear experimental signal difficult to obtain. Even the existence as a bound state, described as a pole in the S-matrix, was debated for decades. Only recently new experimental data coming from BES [11] and KLOE [12] combined with the application of a modified Roy-equation [13, 14] technique asserted the existence of the σ meson.

The mass of the $\sigma/f_0(500)$ was found to be $m_\sigma = 450 + i280 \text{MeV}$ [13, 14] and the particle has been promoted to a proper member of the PDG again [15]. While the existence of the $f_0(500)$ seems beyond doubt, its interpretation in terms of its internal structure is still a matter of debate. Several approaches, including effective theory and large N_c studies [16 − 21] as well as more recent lattice calculations [22, 23], indicate a strong contribution from a $qq\bar{q}\bar{q}$-like operator.

In this contribution we report on our study of tetraquarks within an approach using a covariant four-body equation, which we approximate by a diquark and meson constituent picture. These
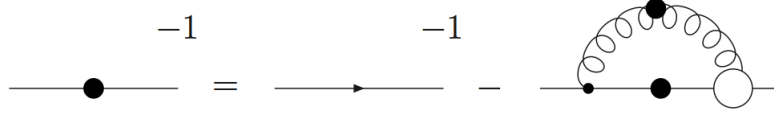
Figure 1: The Dyson-Schwinger equation for the fully dressed quark propagator.

are determined self-consistenly from the the underlying quark and gluon substructure employing a model for the quark-gluon interaction known to reproduce hadron properties on a phenomenological level [24].

2. Meson form factors

2.1 Dyson-Schwinger and Bethe-Salpeter equations beyond rainbow-ladder

The Dyson-Schwinger equation (DSE) for the quark propagator is given diagrammatically in Fig. 1. On the left-hand side we find the fully dressed inverse quark propagator $S^{-1}(p) = i\not{p}A(p^2) + B(p^2)$. The first term on the right-hand side denotes its bare counterpart $S_0^{-1}(p) = i\not{p} + m$, and the self-energy includes again the fully dressed quark propagator as well as the gluon propagator and a bare and a dressed quark-gluon vertex.

For phenomenological purposes, a commonly used approximation scheme for the coupled system of the quark DSE and Bethe-Salpeter equation (BSE) is the rainbow-ladder approach. In the quark DSE this approximation amounts to the simple choice of $\Gamma(p,q)_\mu = \gamma_\mu \Gamma(k)$ for the quark-gluon vertex, where p and q are the ingoing and outgoing quark momenta and k is the momentum of the gluon. This approximation ignores further tensor structures of the full vertex as well as the dependence of the dressing function on the quark momenta. The remaining dressing $\Gamma(k)$ can then be combined with the dressing $Z(k)$ of the Landau-gauge gluon propagator,

$$D_{\mu\nu}(k) = \left(\delta_{\mu\nu} - \frac{k_\mu k_\nu}{k^2}\right)\frac{Z(k^2)}{k^2}, \tag{2.1}$$

into a single effective coupling for the quark-gluon interaction. The most important property of this approximation is that it readily allows for the construction of a corresponding interaction kernel in the Bethe-Salpeter equation of mesons, thus satisfying the axial-vector Ward-Takahashi identity (axWTI). This is mandatory to obtain the pion in the chiral limit as both, a Goldstone boson and a bound state of a massive quark-antiquark pair.

Although there is much phenomenological success in describing mass spectroscopy of light hadrons, decay constants [25–27] and dynamical properties like meson form factors [28] with good agreement to experiment [29], the rainbow-ladder scheme is not sufficient when it comes to the inclusion of unquenching effects like pion-cloud contributions. In the tower of coupled Dyson-Schwinger equations, such contributions appear already in the DSE for the quark-gluon vertex, see [9] for details. When these contributions are taken into account explicitly, the resulting quark-gluon interaction can be split into a pure Yang-Mills part (present already in the quenched approximation) and a separate part denoting the effects of the back-reaction of pions onto the quark propagator. The DSE is then given diagrammatically in Fig. 2 [9]. The corresponding equation is
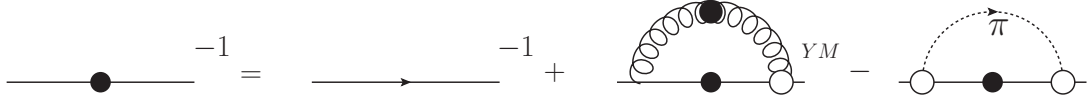
Figure 2: Dyson-Schwinger equation for quark propagator with explicit diagram for the pion back-reaction.

given by

$$
S^{-1}(p) = Z_2 S_0^{-1}(p) + g^2 C_F (Z_2)^2 \int \frac{d^4k}{(2\pi)^4} \gamma_\mu S(k) \gamma_\nu \left(\delta_{\mu\nu} - \frac{q_\mu q_\nu}{q^2} \right) \frac{Z(q^2)\Gamma_{YM}(q^2)}{q^2}
$$
$$
- \frac{3}{2} \int \frac{d^4k}{(2\pi)^4} \left[Z_2 \gamma_5 S(k) \Gamma_\pi \left(\frac{p+k}{2}; k-p \right) + Z_2 \gamma_5 S(k) \Gamma_\pi \left(\frac{p+k}{2}; p-k \right) \right] \frac{D_\pi(q^2)}{2}, \tag{2.2}
$$

with the momentum routing $q = p - k$ and the pion propagator $D_\pi(q^2) = 1/(q^2 + M_\pi^2)$. The product $Z(k^2)\Gamma_{YM}(k^2)$ stands for the Yang-Mills part of the quark-gluon interaction, which we approximate in the spirit of the rainbow-ladder approach. The Maris-Tandy model [27] that parametrizes $Z(k^2)\Gamma_{YM}(k^2)$ is given by:

$$
Z(k^2)\Gamma_{YM}(k^2) = \frac{4\pi}{g^2} \left(\frac{\pi}{w^6} D k^4 exp(-k^2/w^2) + \frac{2\pi\gamma_m [1 - exp(-q^2/4m_t^2)]}{log(\tau + (1 + k^2/\Delta_{QCD}^2))} \right), \tag{2.3}
$$

with $m_t = 0.5\,GeV$, $\tau = e^2 - 1$, $\gamma_m = 12/(33 - 2N_f)$ and $\Delta_{QCD} = 0.234\,GeV$. In the pion part of the interaction, $\Gamma_\pi(p;P)$ is the full pion wave function which we approximate by its leading amplitude in the chiral limit [25]:

$$
\Gamma_\pi^j(p;P) = \tau^j \gamma_5 \frac{B_\chi(p^2)}{f_\pi}. \tag{2.4}
$$

Here, $B_\chi(p^2)$ is the scalar dressing function of the quark propagator in the chiral limit. The replacement of the leading physical pion amplitude by this chiral-limit approximation is correct on the few-percent level. Note that we use this approximation only for the internal pion which mediates the interaction.

The Bethe-Salpeter equation for meson bound states is shown diagrammatically in Fig. 3. The corresponding equation reads:

$$
\Gamma_{tu}^{(\mu)}(p;P) = \int \frac{d^4k}{(2\pi)^4} \left(K_{tu;rs}^{YM}(p,k;P) + K_{tu;rs}^{pion}(p,k;P) \right) \left[S(k_+) \Gamma^{(\mu)}(k;P) S(k_-) \right]_{sr}, \tag{2.5}
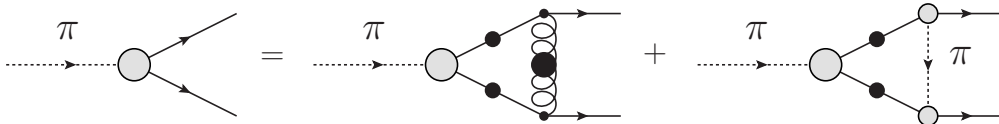$$

Figure 3: Bethe-Salpeter equation for quark anti-quark bound state with explicit diagram for the pion back-reaction.

4

with the kernels $K_{tu;rs}^{YM}$ and $K_{tu;rs}^{pion}$ given by:

$$K_{tu;rs}^{YM}(p,k;P) = \frac{g^2 Z(q^2)\Gamma^{YM}(q^2)(Z_2)^2}{q^2}\left(\delta_{\mu\nu} - \frac{q_\mu q_\nu}{k^2}\right)\left[\frac{\lambda^a}{2}\gamma_\mu\right]_{ts}\left[\frac{\lambda^a}{2}\gamma_\nu\right]_{ru}, \quad (2.6)$$

$$K_{tu;rs}^{pion}(p,k;P) = \frac{1}{4}[\Gamma_\pi^j]_{ru}\left(\frac{p+k-P}{2};p-k\right)[Z_2\tau^j\gamma_5]_{ts}D_\pi(q^2)$$

$$+ \frac{1}{4}[\Gamma_\pi^j]_{ru}\left(\frac{p+k-P}{2};k-p\right)[Z_2\tau^j\gamma_5]_{ts}D_\pi(q^2)$$

$$+ \frac{1}{4}[\Gamma_\pi^j]_{ru}\left(\frac{p+k+P}{2};p-k\right)[Z_2\tau^j\gamma_5]_{ts}D_\pi(q^2) \quad (2.7)$$

$$+ \frac{1}{4}[\Gamma_\pi^j]_{ru}\left(\frac{p+k+P}{2};k-p\right)[Z_2\tau^j\gamma_5]_{ts}D_\pi(q^2).$$

Here, $\Gamma^{(\mu)}(p;P)$ is the Bethe-Salpeter vertex function of a quark-antiquark bound state. The Latin indexes (t,u,r,s) of the kernels refer to their Dirac structure. It has been shown explicitly in [8] that this interaction kernel satisfies the axWTI.

2.2 Coupling the meson bound state to an external field

A systematic procedure to couple bound states to external gauge fields was given by [30] and applied to the diquark-quark model of baryons in Ref. [31] and to the three-body Faddeev equation in Refs. [6, 32]. In short, the evolution of the two-body quark system is given by the amputated version of the scattering matrix T. This function can be obtained by solving a Dyson equation:

$$T = -iK - iKG_0T, \quad (2.8)$$

where G_0 is the disconnected product of two full quark propagators and $-iK$ is the two-quark interaction kernel. When the two-quark system forms a bound state, the scattering matrix develops a pole at $P^2 = -M^2$, and can be defined as:

$$T \approx \frac{\Gamma\bar{\Gamma}}{P^2+M^2}. \quad (2.9)$$

Substituting (2.9) in (2.8) and keeping only the singular term, we arrive at the Bethe-Salpeter equation for the two-quark bound state:

$$\Gamma = -iKG_0\Gamma. \quad (2.10)$$

Then a systematic coupling to the external gauge field gives for $T^{(2)}$:

$$T^\mu = T(iK^{-1}K^\mu K^{-1} + G_0^\mu)T. \quad (2.11)$$

The bound-state electromagnetic current J^μ can be expressed at the pole by:

$$T^\mu \approx \frac{\Gamma_f}{P_f^2+M_f^2}J^\mu\frac{\bar{\Gamma}_i}{P_i^2+M_i^2}. \quad (2.12)$$

Substituting this in (2.11) and using (2.10), we get:

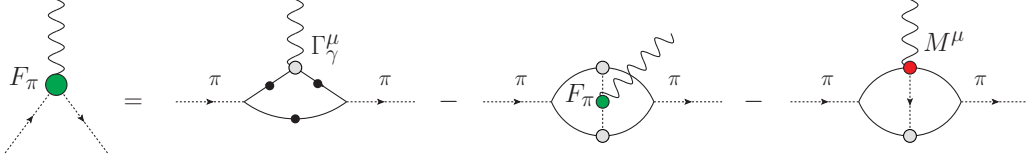$$J^\mu = \Gamma_f(-iG_0K^\mu G_0 + G_0^\mu)\Gamma_i. \quad (2.13)$$

Figure 4: The pion form factor. All internal vertexes and propagators are dressed.

So far, in rainbow-ladder approximation the first term $K_{RL}^\mu = K_{RL}^{(2),\mu} = 0$ because the gluon does not couple to a photon. Including the pion back-coupling, however, the gauged kernel does contribute, since the photon can couple to the exchanged pion. This fact generates two additional diagrams for the pion form factor, which are given in Fig. 4. Here M^μ is an ansatz for the pion-quark-quark-photon-vertex, which can be built along the corresponding one for the diquark-quark-quark-photon vertex derived in [31]. It reads:

$$M^\mu = q_q \frac{(4(p-q)-Q)^\mu}{4(p-q)\cdot Q - Q^2} \left(\Gamma((p-q)-Q/2) - \Gamma(p-q)\right)$$
$$+ q_{ex} \frac{(4(p-q)-Q)^\mu}{4(p-q)\cdot Q - Q^2} \left(\Gamma((p-q)+Q/2) - \Gamma(p-q)\right). \tag{2.14}$$

In comparison to rainbow-ladder, the calculation becomes more complicated. For example, the second diagram involves the pion form factor itself, so that will lead to the necessity to perform a self-consistent, iterative calculation which is also complicated by the two-loop integration.

Up to now we have performed only a part of the calculation, namely the first diagram in Fig. 4. The resulting pion form factor with pion back-coupling is shown in Fig. 5. Although the general
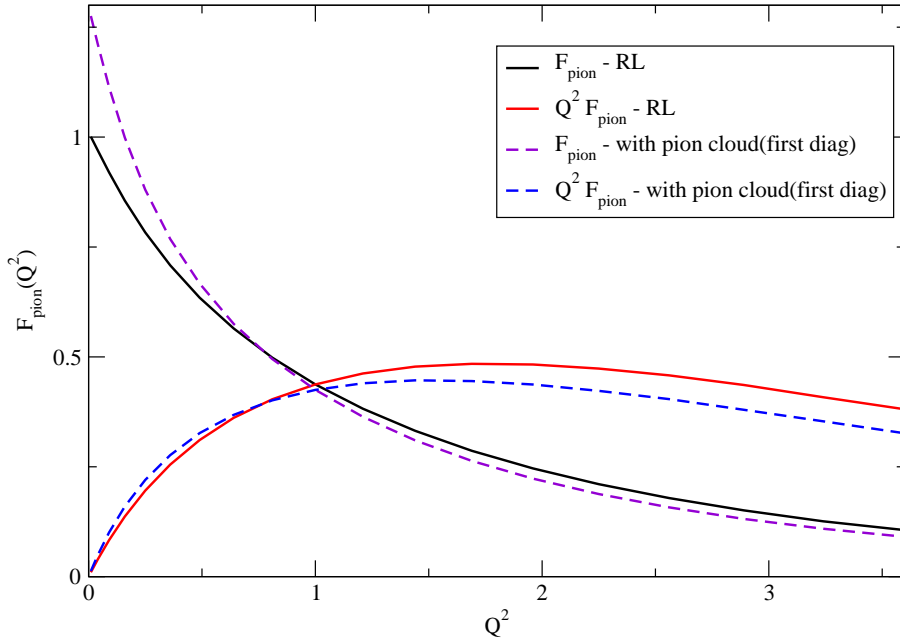

Figure 5: The comparison of pion form factors within rainbow-ladder truncation and with pion back-coupling included.

behavior of the form factor is already satisfying, we observe sizable deviations from one at zero momentum transfer. This violation of current conservation stems from the omission of the pion exchange as well as the seagull diagram in Fig. 4 and may indicate the size of corrections to be expected from these contributions. We are currently in the process of completing the calculation of the two remaining diagrams. In the future we expect to be able to extend the framework to other light- and heavy-meson channels as well as into the baryon sector.

3. Tetraquarks

3.1 Bethe-Salpeter equation for the tetraquark

Bound states can be characterized as poles in the appropriate n-point Green function. The amplitude and the mass of a bound state are found by solving a Bethe-Salpeter equation [34]. The general structure of a multi-particle Bethe-Salpeter equation and especially the tetraquark BSE can be found in [35, 36]. They have the common structure:

$$\Psi = K G_0 \Psi. \tag{3.1}$$

Ψ denotes the amplitude of the tetraquark bound-state, K is the four-body interaction kernel and G_0 represents a product of four fully-dressed quarks. The multiplication is defined in a functional sense and assumes implicit integration of all intermediate momenta and Dirac, color and flavor indices. Following the successful strategy in the baryon sector [37], we drop all 3PI and 4PI contributions. The resulting truncated kernel is a sum of the three remaining pair interactions [36]:

$$K = \sum_{aa'} K_{aa'} \quad \text{and} \quad K_{aa'} = K_a + K_{a'} - K_a K_{a'}. \tag{3.2}$$

The subscripts a and a' denote $q\bar{q}$, qq and $\bar{q}\bar{q}$ pairs, respectively. In principle Eq. (3.1) can now be solved with the same techniques used for the nucleon [38]. This is, however, a numerically demanding undertaking and therefore a reduction to a two-body system is employed.

The construction of an appropriate 2-body system involves the pair-interacting scattering T-matrix

$$T_{aa'} = T_a + T_{a'} + T_a T_{a'} \tag{3.3}$$

which is closely related to the interaction kernels via Dyson's equation:

$$T_{aa'} = K_{aa'}(1 + T_{aa'}) \quad \text{and} \quad T_a = K_a(1 + T_a), \tag{3.4}$$
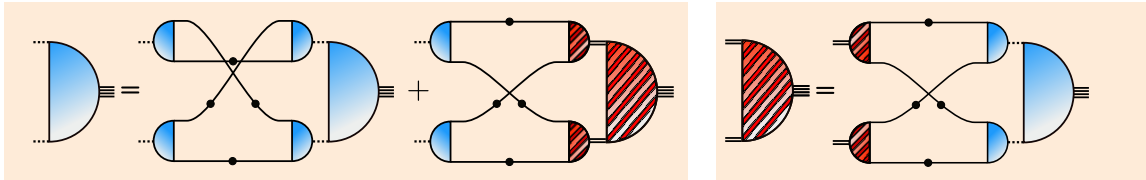

Figure 6: Tetraquark BSE in the meson-meson/antidiquark-diquark picture. The hatched amplitudes involve diquark quantities; the remaining ones are of mesonic nature. Single (double, dashed) lines are dressed quark (diquark, meson) propagators.

where we drop the first two terms in Eq. (3.3). It is important to note that the two-body scattering matrix T_a contains a pole of either a meson or diquark:

$$T_a = -\Gamma_a D_a \bar{\Gamma}_a, \tag{3.5}$$

where Γ is the meson or diquark amplitude and D the corresponding propagator. These pole contributions are assumed to be dominant. The key idea in the construction of a two-body equation is now the substitution of the interaction kernels with the T-matrices in a pole approximation. This ensures the BSE to be expressed in previously calculated degrees of freedom: mesons, diquarks and quarks.

Putting everything together, the BSE in Eq. (3.1) reduces from a four-body equation, featuring quarks with gluons as exchange particles, to an effective two-body equation. The constituents are now mesons and diquarks interacting via quark exchange, see Fig. 6. We take into account only the mesons and diquarks with lowest mass, expecting the higher-mass state contributions to be subleading. It is interesting to note that our approach does not permit a pure diquark-antidiquark state. Combining both equations in Fig. 6 renders diquark-antidiquark contributions to appear internally only. Thus, one may view the resulting tetraquark bound state as a meson molecule with diquark-antidiquark admixture to its kernel.

3.2 Results and Discussion

Our result [39] for the mass of the up/down 0^{++} tetraquark state as a function of the pseudoscalar-meson mass is shown in the left panel of Fig. 7, together with a calculation that only includes the meson-molecule component of the tetraquark. The line represents a fit to the data including a constant, a square root and a linear term. Besides favoring a $\pi\pi$-molecule picture over a subleading diquark-antidiquark component, the main result of our investigation is the value for the u/d tetraquark at the physical point with $m_{PS} = m_\pi$:

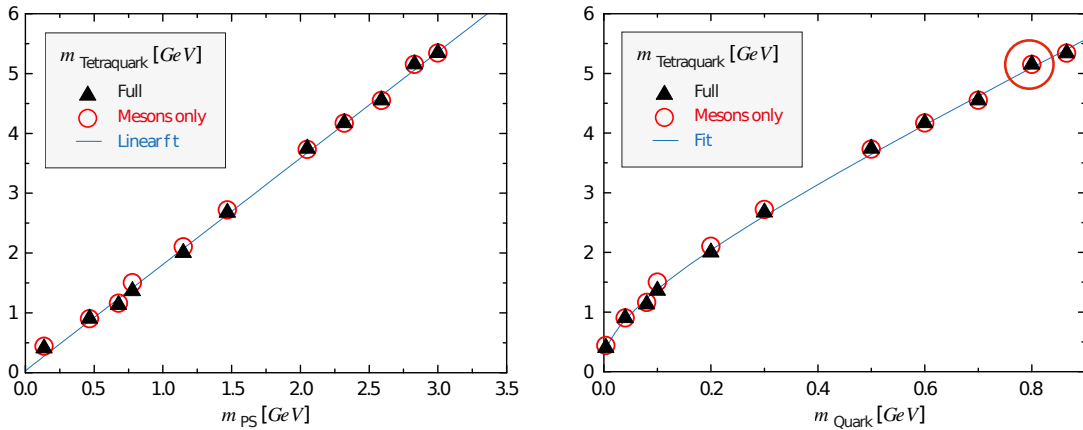$$m_T^{u/d}(0^{++}) = 403\,\text{MeV}. \tag{3.6}$$

Figure 7: Mass of the 0^{++} tetraquark as a function of the pseudoscalar-meson mass (left) and the quark mass [39]. The large red circle highlights a potential all-charm tetraquark.

This value is somewhat lower than the mass deduced from the Roy-equation [13, 14] but other bound states that can mix with the scalar tetraquark are not included in our work. The behavior of the tetraquark mass in dependence of the quark mass shows some interesting features: Except for the chiral mass region, the fit resembles the typical behavior of a Goldstone boson. This can be readily understood from the strongly dominating meson-meson component to the tetraquark bound state. Furthermore, the large decay constant and the low mass of the σ is in accordance with our picture of a $\pi\pi$-molecule dominated tetraquark.

It is furthermore interesting to speculate about the existence of an all-charm tetraquark state. In Fig. 7 the largest pseudoscalar-meson mass corresponds to a quark mass in the charm region. We therefore read off the mass of an all-charm scalar tetraquark state to be at

$$m_T^c(0^{++}) = 5.3\,\text{GeV}. \tag{3.7}$$

This mass is considerably lower than the 6.2 GeV which were obtained in simpler model calculations [40, 41]. It is also much lower than the η_c threshold. Potential decay channels into D mesons and pairs of light mesons necessarily involve internal gluon lines. This could result in rather small decay widths. Further results for tetraquarks with different quantum numbers are in progress.

Acknowledgements

References

[1] P. Maris and C. D. Roberts, Int. J. Mod. Phys. E **12** (2003) 297.

[2] C. S. Fischer, J. Phys. G **32** (2006) R253.

[3] P. Maris and P. C. Tandy, Nucl. Phys. Proc. Suppl. **161** (2006) 136.

[4] G. Eichmann, I. C. Cloet, R. Alkofer, A. Krassnigg and C. D. Roberts, Phys. Rev. C **79** (2009) 012202.

[5] A. W. Thomas, S. Theberge and G. A. Miller, Phys. Rev. D **24** (1981) 216.

[6] G. Eichmann, Phys. Rev. D **84** (2011) 014014.

[7] G. Eichmann and C. S. Fischer, Eur. Phys. J. A **48** (2012) 9.

[8] C. S. Fischer, D. Nickel and J. Wambach, Phys. Rev. D **76** (2007) 094009;
C. S. Fischer, D. Nickel and R. Williams, Eur. Phys. J. C **60** (2009) 47.

[9] C. S. Fischer and R. Williams, Phys. Rev. D **78** (2008) 074006.

[10] R.L. Jaffe, Phys.Rev. D15 (1977) 281.

[11] M. Ablikim *et al.* [BES Collaboration], Phys. Lett. B 598 (2004) 149.

[12] A. Aloisio *et al.*, Phys. Lett. B 537 (2002) 21.

[13] I. Caprini, G. Colangelo and H. Leutwyler, Phys. Rev. Lett. 96 (2006) 132001.

[14] R. Garcia-Martin, R. Kaminski, J. R. Pelaez and J. Ruiz de Elvira, Phys. Rev. Lett. 107 (2011) 072001.

[15] K. Nakamura *et al.* [Particle Data Group Collaboration], J. Phys. G 37 (2010) 075021.

[16] E. Santopinto and G. Galata, Phys. Rev. C 75 (2007) 045206.

[17] N. N. Achasov and V. N. Ivanchenko, Nucl. Phys. B 315 (1989) 465.

[18] D. Black, A. H. Fariborz, F. Sannino and J. Schechter, Phys. Rev. D 59 (1999) 074026.

[19] F. Giacosa, Phys. Rev. D 74 (2006) 014028; Phys. Rev. D 75 (2007) 054007.

[20] E. Klempt and A. Zaitsev, Phys. Rept. 454 (2007) 1.

[21] D. Ebert, R. N. Faustov and V. O. Galkin, Eur. Phys. J. C 60 (2009) 273.

[22] N. Mathur *et al.*, Phys. Rev. D 76 (2007) 114505.

[23] S. Prelovsek, Acta Phys. Polon. Supp. 3 (2010) 975.

[24] P. Maris and C. D. Roberts, Int. J. Mod. Phys. E 12 (2003) 297;
P. Maris and P. C. Tandy, Nucl. Phys. Proc. Suppl. 161 (2006) 136.

[25] P. Maris, C. D. Roberts and P. C. Tandy, Phys. Lett. B 420 (1998) 267.

[26] P. Maris and C. D. Roberts, Phys. Rev. C 56 (1997) 3369.

[27] P. Maris and P. C. Tandy, Phys. Rev. C 60 (1999) 055214.

[28] P. Maris and P. C. Tandy, Phys. Rev. C 62, 055204 (2000).

[29] J. Volmer et al. [The Jefferson Lab F_π Collaboration], Phys. Rev. Lett. 86, 1713 (2001).

[30] A. N. Kvinikhidze and B. Blankleider, Phys. Rev. C 60 (1999) 044003.

[31] M. Oettel, M. Pichowsky and L. von Smekal, Eur. Phys. J. A **8** (2000) 251.

[32] G. Eichmann and C. S. Fischer, Phys. Rev. D **87** (2013) 036006.

[33] R. L. Jaffe, Nucl. Phys. Proc. Suppl. 142 (2005) 343; A. Selem and F. Wilczek, hep-ph/0602128.

[34] E. Salpeter, H. Bethe, Phys.Rev. 84 , (1951) 1232.

[35] K. Huang, H. A. Weldon, Phys.Rev. D11 257 (1975) 275.

[36] A. Khvedelidze, A. Kvinikhidze, Theor.Math.Phys. 90 (1992) 62.

[37] G. Eichmann, R. Alkofer, A. Krassnigg and D. Nicmorus, Phys. Rev. Lett. 104 (2010) 201601.

[38] G. Eichmann, Phys. Rev. D 84 (2011) 014014.

[39] W. Heupel, G. Eichmann, C.S. Fischer, Phys. Lett. B 718 (2012) 545.

[40] Y. Iwasaki, Prog. Theor. Phys. **54** (1975) 492.

[41] R. J. Lloyd and J. P. Vary, Phys. Rev. D **70** (2004) 014009.